

RSC Advances



This is an *Accepted Manuscript*, which has been through the Royal Society of Chemistry peer review process and has been accepted for publication.

Accepted Manuscripts are published online shortly after acceptance, before technical editing, formatting and proof reading. Using this free service, authors can make their results available to the community, in citable form, before we publish the edited article. This *Accepted Manuscript* will be replaced by the edited, formatted and paginated article as soon as this is available.

You can find more information about *Accepted Manuscripts* in the [Information for Authors](#).

Please note that technical editing may introduce minor changes to the text and/or graphics, which may alter content. The journal's standard [Terms & Conditions](#) and the [Ethical guidelines](#) still apply. In no event shall the Royal Society of Chemistry be held responsible for any errors or omissions in this *Accepted Manuscript* or any consequences arising from the use of any information it contains.

Optical Response of Nanoclusters under Confinement

Balasaheb J. Nagare¹

Department of Physics, University of Mumbai, Santacruz (East), Mumbai-400 098, India. ^{a)}

We report optical properties of metallic and semiconductor nanoclusters with various sizes as a function of confinement using real-space time dependent density functional theory (TDDFT). The lowest equilibrium structures have been selected by examining the evolution of lowest five isomers for each cluster as a function of volume for six different compression. The minimum volume considered is about $1/10^{th}$ of the free space box volume. The absorption spectra depict a blue shift, an increase in intensity and change in line shape of the spectral lines of a confined systems. The observed enhanced intensity of spectral lines is found to be about two to three fold at high compression as compared to its counterpart. This is accompanied by an increase in the optical band gap and excitation energy of transitions with compression. In all the systems that we investigate, the observed blue shift, an enhanced intensity and a change in line shape of the spectral lines are found to be generic in nature.

^{a)}Electronic mail: bjnagare@gmail.com

INTRODUCTION

It is well established that geometrical confinement modifies the properties of materials. Confinement could be due to a surface, an interface, an adsorbent layer or encapsulation in nanotubes. Such materials often display unusual structure^{1,2} and new physiochemical properties.³⁻⁵ Therefore, considerable efforts have been directed towards elucidating the properties of such systems under confinement. Confinement may change the geometric arrangement of atoms accompanied by significant changes in the electronic energy levels leading to very different structural, electronic, magnetic, and optical properties. Among it, we select optical properties of materials due to their advanced technological applications. Previously, it has been widely used to enhance the surface sensitivity of several spectroscopic measurements, including fluorescence, analysis of biomolecular interactions, optical waveguides and in the areas of materials science because of its real-time, label-free, and noninvasive nature⁶.

During the last two decades, both extensive experimental and theoretical studies have been carried out on optical properties of small and medium-sized sodium clusters. Although early interests were mainly in the size- and geometry-dependence of the absorption spectra, several authors have discussed the electronic excitations in these spectra. Selby et.al⁷ have measured photoabsorption cross section in the wavelength range of 452–604 nm. They have observed single surface resonance plasmon peaks in a closed shell and double or triple peaks in open shell clusters. These findings have further supported by the ellipsoidal shell model. Recently, Pal et. al.⁸ have used Bethe-Salpeter equation to calculate absorption spectra of closed-shell sodium clusters and their results are in excellent agreement with experiment. Although the optical absorption in alkali metal clusters has been studied by many authors at various levels of theory, however a very few reports of optical absorption in aluminium clusters exist. As far experimental studies of excitation properties in aluminium clusters are concerned, few studies have been performed on Al₂ and Al₃.⁹ Nevertheless, no experimental measurements of optical properties of larger aluminium clusters have been performed.

Due to recent technological advances in the synthesis and characterization techniques of nanomaterials, the current research on metallic and semiconductor nanoclusters have made significant progress in the last a few years, both theoretically and experimentally. It is worth to mention that the surface plasmon resonance is collective effect and observable in the large nanoclusters. Recently, Philip et. al.¹⁰ have shown that when the size of the gold clusters grows above 2 nm, it shows the optical nonlinearity from the nonplasmonic

regime to the plasmonic regime. The encapsulation of gold nanoparticles using thiol molecules has shown the strong confinement of electrons in the clusters.¹¹ Yu et. al.¹² have also been observed the extraordinary optical, electronic and magnetic properties in metallic nanoclusters due to the enhanced quantum confinement. Harb et.al. have been carried out theoretical and experimental investigations of the absorption spectra of Ag clusters embedded in the Ar matrix.¹³ It is found that the blue shift of spectral lines is due to confinement of valence electrons.

It should be mentioned that the present work is carried out within the framework of Casida's Formulation of linear response TDDFT. This approach is universal and in principle capable of producing the exact excitation energies of any systems and material, provided that XC effects are properly accounted for. In the majority of calculations, TDDFT method have been successfully applied to study the optical excitations in finite systems which uses the adiabatic local density approximation (LDA) or time-dependent (TDLDA). It works better in case of finite systems, where generally the shape of the calculated absorption peaks agrees reasonably well with the experimental findings.^{14,15} It is further noted that for large systems, the numerical scaling of TDDFT in the Casida formalism to N^3 versus N^5 for wavefunction methods of comparable accuracy (eg. CCSD, CASSCF). Previously, it has successfully been used to obtain excitation energies in many finite systems. Recently, Weissker et. al has used it successfully to calculate the optical response in quantum-sized Ag and Au clusters.¹⁶ Even though this formalism allows to compute Born-Oppenheimer hypersurfaces for excited states and identify well-separated excitation eigenenergies for finite systems but failed for extended systems such as bulk, periodic chains and slabs.

Thus, many studies have been reported to understand optical excitations in free clusters. However, a model calculation on the optical spectra of an isotropically compressed cluster has never been done. In the present work, we calculate the optical properties of clusters at the center of an inert and the impenetrable cubical box. Our interest in this arose from the more general question of how the optical spectra of the clusters differ from its free state, when the atom is in a physically interesting environment (e.g., in a solid matrix or liquid, in a micropore, or near a wall). We understand the role of compression on optical excitations by raising some interesting questions; (i) Whether sodium clusters would show the optical transitions under compression as it have been observed in sodium bulk at 200 GPa¹⁷? (ii) Does there a characteristic difference in the optical absorption as compared with free space? (iii) What is the nature of the shift of the spectral lines with compression? (iv) How does the inclusion of confinement affect intensity of spectral lines? and finally (v) Whether observed trends would show the same pattern in the other systems with

similar valence electronic structure?

To gain insight into some of these questions, we have carried out systematic real-space TDDFT calculations on a series of sodium clusters in the size range of $N = 2$ – 20 . These clusters are isotropically compressed into hard-walled three-dimensional cubic box. The walls are hard in the sense, wavefunctions go to zero at the wall. We also extend this study to few lowest equilibrium isomers of sodium clusters. To verify the observed trends in the optical response of these clusters, we also extend this study to other systems with similar valence electronic structures, namely Li_8 , K_{10} , and Cs_7 . Further, to see the generic nature of the optical response of clusters, we extend it to some metallic and semiconductor nanoclusters such as Ag_2 , Au_2 , Al_{13} and Si_8 . We bring out the evolution of optical spectra, role of hybridization and molecular orbitals under confinement and compare with free space results. Finally, we explain the generic nature of the optical absorption which is observed in all systems under high compression.

The rest of this article is organized as follows. In the next section, we describe the model and technical details of our simulations. Section III present and discuss the results of our calculations. Finally, in section IV, we summarize our results along with some important concluding remarks.

COMPUTATIONAL DETAILS

The optical property calculations have been performed using TDDFT method implemented in OCTOPUS code.¹⁸ All self and non-self consistent calculations (SCF and NSCF) have been carried out with generalized gradient approximation (GGA) given by Perdew–Burke–Ernzerhof (PBE)¹⁹, except in the Casida calculations, where the available kernel in OCTOPUS corresponds to LDA. Troullier-Martins pseudopotentials²⁰ were used in all of the TDDFT calculations in this work. We also note that spin polarization has been taken into account, if the number of electrons is odd.

The ground state and lowest equilibrium clusters used in this study have been obtained by a simulated annealing method. The resulting structures have been re-optimized with density functional theory as described below. Among it, we have selected first six lowest isomers for confinement study. It should be noted that free sodium clusters in this size range have been extensively studied. In all the cases, the geometries of all the lowest energy structures in free space are in good agreement with the results of the published data.²¹ In each of the cases, the six isomers are subjected to various compressions by a hard-walled three dimensional cubic boxes whose volume (V) were reduced from V_0 to $V/V_0 = 0.05$, where, V_0 is the volume

of a cubic box corresponding to free space. In case of large clusters, it was reduced up to $V/V_0 = 0.125$. We denote the smallest volume by V_h .

The geometry optimizations of the clusters have been performed using the OCTOPUS code. All optimized geometries were considered to be converge when the change in energy was of the order of 10^{-5} hartrees and the absolute maximum force was less than 0.002 hartrees/Å. A grid spacing of 0.18 Å for the real space grid have been used for all calculations. The validity of the grid-spacing have been verified by reference calculations for the test structure Na₂ using grid-spacings of 0.09 to 0.30 Å. All five grid-spacings 0.16 to 0.20 Å have reproduced similar absorption spectra up to an accuracy of about 0.1 eV in the relevant low-energy region of about 0-6 eV.

To calculate absorption spectra, we have applied Casida's formalism implemented in TDDFT method.^{22,23} Following a ground state, SCF calculation, an NSCF were performed with a large number of unoccupied orbitals. In the Casida's calculations, the accuracy of results depends on the number of unoccupied states. The number of the unoccupied states that were taken into account was 4 times the number of occupied states in the smaller clusters and at least 8 times the number of occupied states for the medium-sized clusters. These numbers are selected in a such way that the optical absorption spectrum extends up to the first ionization potential value of the cluster which are under considerations.

We have verified the accuracy of our model on the Na₂ molecule. We find a bond length of 3.16 Å and ionization potential of 5.21 eV. These results are comparable to experimental value reported by Huber et. al.²⁴ We have also verified the accuracy of excited state calculations. It shows three major resonance peaks at 1.87, 2.57 and 3.87 eV which is in good agreement with the experimental data.²⁵

RESULTS AND DISCUSSION

We have investigated the effect of compression on optical response of metallic and semiconductor nanoclusters. First we have examined the absorption spectra of a series of lowest equilibrium structures of Na_n clusters with n=2-20. In each of the cases, we have used five to seven different volumes depending on the size of the cluster. As we shall see in many of the cases, it is most convenient to bring out the effect of compression by comparing the results for free space volume (V_0)²⁶ with highest compression volume (V_h). We further examine the optical response of few lowest equilibrium isomers of sodium to confirm whether the nature of absorption spectra shows similar trends. We then extend this study to the systems with similar

valence electronic structure, namely Li_8 , K_{10} and Cs_7 clusters to verify the observed trends in the absorption spectra of sodium clusters under confinement. Finally, we examine the optical response in some of metallic and semiconductor nanoclusters such as Au_2 , Ag_2 , Si_8 , Al_{13} to see the generic nature of observed results in the above systems. The optimized geometries of the lowest equilibrium structures of all systems at V_0 and V_h are shown in Figure 1. We will first present the results on optical properties. This is followed by a discussion on eigenvalue spectrum and transitions between the excited states along with some relevant molecular orbitals to understand the origin of optical excitations under high compression.

For the sake of completeness, we note certain salient features sodium clusters in confined space geometries. All sodium clusters do not show significant change unless the volume is reduced to about 70% of free space box volume. Thereafter the change in total energy, kinetic energy and other components show highly nonlinear behaviour. The change in the kinetic energy has most dominated. The geometries tend to become more spherical. In most of the cases, the HOMO-LUMO gap reduces mainly due to the change in the ground state geometries. However, In few cases Na_2 , Na_5 , Na_7 and Na_8 , where the ground state geometries remain unchanged, HOMO-LUMO gap increases as expected from the simple particle in a box model. We observe that the strong confinement leads to significant isomeric transitions.²⁷

In Table I and II, we summarize in detail the electronic states giving rise to the most intense absorption features, in order to identify the nature of the photoabsorption transitions in terms of electronic structure of sodium clusters in free and confined geometry, respectively. It show the ionization potential (I.P.), excitation energy of major transitions (E_{exc}), energy of the most significant peak (E_m), strength function (S_ω), HOMO-LUMO gap (E_g), optical band gap (E_{gopt}) and excited state compositions. The number of features can be discerned from the Tables: (1) The inclusion of confinement significantly reduces the ionization potential due to overlap of electronic orbitals and confined-induced strong coulombic repulsion. The calculated values of ionization potential in the free space are in reasonable agreement with the experimental data.^{28,29} (2) In the majority of clusters, the first major excitation occurs in the energy range between 3 to 5 eV. However, in case of free clusters, it lies in between 2 to 3 eV. (3) The optical absorption peak smoothly shifts to higher energies. (4) The confinement also induces the decrease in the number of absorption bands as compared with absorption spectra at V_0 . (5) The increase in oscillator strength with compression is about to 2 to 3 fold and substantial gains in E_{gopt} as compared with its counterpart. Thus, above observations enable us to rationalize the notable difference in the character of the electronic transitions which are mostly contributing to the absorption peak at V_0 and V_h .

First, we briefly discuss the optical excitations of free clusters which are shown in Figure 2 for the free (V_0) and confined geometries (V_h). Each system shows a similar spectrum with an absorption edge above 2 eV. Several peaks appear with slightly varying pattern depending on the type of structure. We have observed that the intensity of spectral lines increases with increasing cluster size. The occurrence of the number of absorption peaks in the spectra from one to five atoms, but stays more or less constant for larger clusters with no significant change in the fine structure of the spectra of clusters more than five atoms. It is noted that in the majority of the clusters, the first major excitations occur in the energy range between 2 and 3 eV. We have also observed that several spectra depict similar absorption bands. This is in excellent agreement with experimental results.^{7,30} It is worth to note that dipole allowed transitions for free, sodium clusters are reproduced with reasonable accuracy and are compared with the available spectroscopic data.²⁵ For instance, the three major resonance peaks at 1.86, 2.57 and 3.87 eV for Na_2 agrees well with the experimental one within 0.04 eV accuracy; the calculated resonance peaks at 2.70 and 2.88 eV for Na_{20} clusters corresponds to the experimental values.³¹ Further, multiple excitation peaks are also observed, which has been associated with transitions from $3s$ to $3p$, $3d$ and $3p$ to $4s$ levels.³²⁻³⁴ Thus, it has clearly been seen that even though the cluster size increases, the peaks of resonance frequency do not show a monotonous decrease as expected due to quantum confinement effects.

To see the effect of confinement on the optical properties of sodium clusters, we have carried out extensive *ab initio* time dependent density functional calculations on a series of sodium clusters with a size range of $n=2-20$ confined at the center of a hard-walled three-dimensional cubical box. Figure 2 shows a blue shift with an enhancement of the intensity of spectral lines. The enhanced intensity of spectral lines are around three fold at high compression as compared with free space. It also depicts the change of line shape of spectral lines in all cases at V_h with a reduction in the number of peaks. The blue shift of the resonance peaks can be understood from the simple model of a particle in an infinite potential well. Given the relation between energy and momentum, one can see how a series of nearby transitions occurring at slightly different energies can be compressed into a single intense peak in confined system, at least the number of peaks is reduced. Thus, it is observed that the intensity of the spectral lines shows sharp increase, whereas the other small peaks either vanish or reduced significantly indicating a much sharper optical transition. It is interesting to note that the increase in the intensity of spectral lines, up to two to three orders of magnitude compared to that of free clusters with the disappearance of the minor resonance peaks. In addition to these observations, it also depicts the increase in the optical band gap accompanied with excitation energy at high

compression.

Next, we discuss cavity effect on intensities and shift of spectral lines in the absorption spectra. Figure 3 shows a representative case of Na₈ and Au₂ clusters to summarize most relevant findings, as a function of the different compressions. At V₀, the absorption spectra of Au₂ show the transitions with non-vanishing strength function below 7 eV at 2.54, 5.53, 6.17 and 6.68 eV which are comparable to reported results.^{35,36} However, it shifts to higher energy with an increase in the intensity with two fold and this trend continues with the fall of the intensity beyond V_h. The blue shift of spectral lines have been also observed by experiment.³⁷ These observations have been observed in all cases. Thus, it is found that the effects of isotropic compression are effective only after V_c. When the cubical cell volume reaches to V_c, the position of the spectral lines begins to shift to higher energy value with an enhancement in the intensities. This process continues till the compression attains to V_h. The further rise of compression leads to blue shift the frequencies and lowering of the intensities of these lines. Thus, it is observed that the frequencies are all blueshifted. This is as expected, because isotropic compression raises the energies of the upper levels more than it does those of lower levels. Hence, the effect of isotropic compression on these lines is to blue shift the frequencies, while the intensities rise beyond the free cluster values, before falling to decrease for high degrees of compression (beyond V_h). It should be mentioned that the value of V_h is depends on the cluster size.

In order to understand evolution of optical properties of clusters, we examine the nature of eigenvalue spectra shown in Figure 4. It shows the eigenvalue spectra of Na₂, Na₈, Li₈ and K₁₀ in free (left part) and confined space (right part). A number of interesting features can be discerned from the figures such as the formation of the spectra across the series reveals that all energy levels are raised with respect to free-cluster systems, an increase in spacing between the energy levels and this effect is more prominent in the conduction band, breaking of degeneracy of energy levels, exhibit very strong HOMO–LUMO transitions. It is well known that due to quantum confinement, the energy level becomes discrete. The effect of confinement is more effective at higher energy levels since $E \propto n^2/L^2$, where n is the principal quantum number and L is the length of confining box. It shows the more structured pattern at high compression (when the volume reduces below 20% to its original volume). The unoccupied levels split and the gaps become widen. In Na₂, the unoccupied state (LUMO) at -1.80 eV is singlet whereas next to it is doubly degenerate and all unoccupied states are of p-type at V₀. However, at V_h, the state next to HOMO (-1.62 eV), is doubly degenerate (LUMO, LUMO+1) at 1.38 eV. In case of Na₈, the unoccupied levels are bundled into two

groups at V_0 whereas at high compression (V_h), it split into more four groups and the HOMO-LUMO gap is widened. The above observations are also valid for Li_8 and K_{10} clusters. It should be mentioned that GGA underestimates E_g due to inaccuracy in quasi-particle energies and may ultimately be attributed to the inherent lack of derivative discontinuity³⁸ and delocalization error³⁹ in local and semilocal functionals.

We examine in detail the electronic states giving rise to most intense adsorption features, in order to identify the nature of photoabsorption transitions in terms of the electronic structure. For these transitions, we analyze their nature in terms of the leading excited one-electron configurations and, for each excited configuration, the molecular orbitals involved. This analysis is presented in Table I and II for all clusters. Figure 5 and 6 shows a representative case of Na_8 cluster to summarize most relevant findings. At V_0 , the optical absorption spectrum of Na_8 in Figure 2 exhibits a single broad peak extending from 2.45-3.20 eV. It shows pronounced peak at 2.82 eV which is comparable to experimental value.⁴⁰ This transition has dominant contributions from 45.02% $3p_y \rightarrow 4d_{xz}$ (HOMO \rightarrow LUMO+11) and 50.06% $3p_z \rightarrow 4d_{yz}$ (HOMO-1 \rightarrow LUMO+12) configurations. At V_h , the major absorption peak at 3.54 eV shows blue shift as compared to the counterpart. It occurs due to contributions from 15.3% $3p_x \rightarrow 3d_{yz}$ (HOMO-1 \rightarrow LUMO+3), 21.9% $3p_y \rightarrow 4p_x$ (HOMO-1 \rightarrow LUMO+6, forbidden) and 16.7% $3p_z \rightarrow 3d_{xy}$ (HOMO-3 \rightarrow LUMO+1) configurations. The molecular orbital analysis also shows the delocalization of electronic states at high confinement. We further note that the contributions from the excited states reduce substantially, However, the probability of transitions between different states increases.

Further, we have verified the observed trends in the optical excitations in the sodium clusters by extending this study to a few low lying isomeric structures of Na_4 , Na_8 , Na_{10} and Na_{20} . In Figure 7, we show the absorption spectra for the Na_8 and Na_{10} clusters. As mentioned in earlier report²⁶, there is a re-ordering of the isomeric structures when the confinement volume reaches to below the critical volume (V_c). The critical volume is generally reached when the confinement reduces to 50 % of the free cluster volume. However, the value of critical volume depends on cluster size. As expected, in all cases, there are similar trends in the nature of the absorption spectra as mentioned above. Interestingly, we observe the enhancement in intensity of resonance peaks as confining volume is reduced below V_c .

Thus, the effects of confinement seen in bulk¹⁷ have also been shown by the sodium clusters. However, the question is: Whether this enhanced intensity along with blue shift of the spectral lines in the absorption spectra would also be observed in the other systems with similar valence electronic structure? In order to answer this question, we have computed the absorption spectra of Li_8 , K_{10} , Cs_7 as shown in Figure 8. In

case of free Li_8 clusters, the calculated resonance occurs at 2.68 eV which leads to a very good agreement with the experimental value of 2.5 eV.⁴¹ However, at high compression, the spectral line shift to 3.22 eV with a 39% rise in the intensity. For K_{10} cluster, the most intense peak at 2.09 eV shifts to 2.56 eV at high compression with twofold increase in the intensity. The confinement effects in Cs_7 also shows the shift of most intense peak at 1.21 to 1.86 eV with a 34% increase in the intensity as compared to free space.

Finally, we have examined the generic nature of the optical response of clusters by extending this study to some of metallic and semiconductor nanoclusters. We have computed the absorption spectra of Ag_2 , Al_{13} and Si_8 clusters (see Figure 8). In case of free Ag_2 clusters, two major resonance peaks are observed at 3.35 and 4.28 eV which are very close to experimental values at 3.0 and 4.7 eV.⁴² At V_h , these peaks shift to 5.68 and 6.78 eV. It can be added that an increase in the intensity of the spectral lines have doubled as compared with its counterpart. For Al_{13} , three major resonance occurs at 5.99, 7.17 and 7.95 eV at V_0 , which then get pronounced at 11.10 eV at V_h with an enhanced intensity by 25% under highest compression. In free Si_8 cluster, the excitation occurs within energy range 5-15 eV which is in good agreement with TDLDA results reported by Juzar et. al.⁴³ However, we have observed major transitions at 12.95 eV under high compression with enhancement in the intensity by at least two orders of magnitude when compared with free space. Similar enhanced intensity has been observed in silicon nanocrystals due to quantum confinement effects.⁴⁴ Thus, in each of these cases, we do find similar blue shift and an enhanced intensity along with the change of line shapes of spectral lines under high compression.

SUMMARY AND CONCLUDING REMARKS

We have presented results on optical response of metallic and semiconductor nanoclusters as a function of various degrees of isotropic confinement using real space TDDFT method. Firstly, we have examined the evolution of optical excitations in a series of sodium clusters in the size range of 2-20 atoms. Apart from the ground state, we have also calculated the absorption spectra of five low lying isomers. In each of these cases, we have performed the geometry optimizations, SCF and NSCF calculations using the real space DFT method. This is followed by excited state calculations using real space TDDFT (also called as TDLDA) method within Casida's formalism.

The effects of isotropic confinement show many interesting features in the absorption spectra. Our results reveal that free clusters exhibit a more definite dependence of the absorption peaks on the type of structure.

It turns out that the optical absorption spectra of clusters is strongly influenced by the confinement. The optical absorption band smoothly shifts to higher energies, gets relatively broaden, and substantial gains in intensity by increasing compression. The observed blue shift of the spectral lines can be ascribed to the strong repulsive interaction between core and electrons under high compression.

To verify the observed trends in the absorption spectra of sodium clusters and its isomers, we have also examined it to the other systems with similar valence electronic structure, namely Li_8 , K_{10} and Cs_7 clusters. These systems also show similar trends in the absorption spectra, as compared with sodium clusters. To confirm the generic nature of the optical absorption, we have extended this study to Ag_2 , Au_2 , Al_{13} and Si_8 clusters which have also reproduced the similar pattern as seen above. Thus, In all the systems that we investigate, the observed blue shift, an enhanced quantum efficiency and change of line shape of spectral lines are found to be generic in nature.

ACKNOWLEDGEMENT

This research was supported in part by the Department of Science and Technology (DST), through computing resources provided by the high performance computing facility at the Inter University Accelerator Center (IUAC), New Delhi.

REFERENCES

- ¹I. Tamblyn, J.-Y. Raty, and S. A. Bonev. Tetrahedral clustering in molten lithium under pressure. *Phys. Rev. Lett.*, 101:075703, 2008.
- ²M. I. Eremets, I. A. Trojan, S. A. Medvedev, J. S. Tse, and Y. Yao. Superconductivity in hydrogen dominant materials: Silane. *Science*, 319:1506, 2008.
- ³L. F. Lundegaard, G. Weck, McMahon M. I., S. Desgreniers, and P Loubeyre. Observation of an O_8 molecular lattice in the epsilon phase of solid oxygen. *Nature*, 443:201, 2006.
- ⁴L. Gao, Y. Y. Xue, F. Chen, Q. Xong, R. L. Meng, D. Ramirez, C. W. Chu, J. H. Eggert, and H. K. Mao. Superconductivity up to 164 k in $\text{HgBa}_2\text{Ca}_{m-1}\text{Cu}_m\text{O}_{2m+2+\delta}$ ($m=1, 2$, and 3) under quasihydrostatic pressures. *Phys. Rev. B*, 50:4260, 1994.

- ⁵J. S. Tse, Y. Yao, and K. Tanaka. Novel superconductivity in metallic SnH₄ under high pressure. *Phys. Rev. Lett.*, 98:117004, 2007.
- ⁶Karlsson R. J. SPR for molecular interaction analysis: a review of emerging application areas. *Mol. Recognit.*, 17:151–161, 2004.
- ⁷Kathy Selby, Vitaly Kresin, Jun Masui, Michael Vollmer, Walt A. de Heer, Adi Scheidemann, and W. D. Knight. Photoabsorption spectra of sodium clusters. *Phys. Rev. B*, 43:4565, 1991.
- ⁸George Pal, Georgios Lefkidis, Hans Christian Schneider, and Wolfgang Hbner. Optical response of small closed-shell sodium clusters. *J. Chem. Phys.*, 133:154309, 2010.
- ⁹Fu Z., Lemire G. W., Hamrick Y. M., Taylor S., Shui J, and Morse M. D. Spectroscopic studies of the jetcooled aluminum trimer. *J. Chem. Phys.*, 88:3524, 1988.
- ¹⁰Reji Philip, Panit Chantharasupawong, Huifeng Qian, Rongchao Jin, and Jayan Thomas. Evolution of nonlinear optical properties: From gold atomic clusters to plasmonic nanocrystals. *Nano Letters.*, 12(9):4661, 2012.
- ¹¹Rongchao Jin. Quantum sized, thiolate-protected gold nanoclusters. *Nanoscale*, 2:343, 2009.
- ¹²Pyng Yu, Xiaoming Wen, Yon-Rui Toh, Xiaoqian Ma, and Jau Tang. Fluorescent metallic nanoclusters: Electron dynamics, structure, and applications. *Particle and Particle Systems Characterization*, 32(2):142, 2015.
- ¹³M. Harb, F. Rabilloud, D. Simon, A. Rydlo, Lecoultrre, F. Conus, V. Rodrigues, and C. Fèlix. Optical absorption of small silver clusters:Ag_n, (n=422). *J. Chem. Phys.*, 129:194108, 2008.
- ¹⁴Joswig J. O., Tunturivuori L. O., and Nieminen R. M. Photoabsorption in sodium clusters on the basis of time-dependent density-functional theory. *J. Chem. Phys.*, 128:014707, 2008.
- ¹⁵B. Gervais, E. Giglio, E. Jacquet, P. G. Reinhard A. Ipatov, F. Fehrer, and E. Suraud. Spectroscopic properties of Na: clusters embedded in a rare-gas matrix. *Phys. Rev. A*, 71:015201, 2005.
- ¹⁶Hans-Christian Weissker, Robert L. Whetten, and Xochitl Lopez-Lozano. Optical response of quantum-sized Ag and Au clusters cage vs. compact structures and the remarkable insensitivity to compression. *Phys. Chem. Chem. Phys.*, 16:12495, 2014.
- ¹⁷Y. Ma, M. Ermets, A. R. Organov, Y. Xie, I. Trojan, and S. Medvedev. Transparent dense sodium. *Nature*, 458:182, 2009.
- ¹⁸M. A. L. Marques, A. Castro, G.F. Bertsch, and A. Rubio. Octopus: A first-principles tool for excited electron-ion dynamics. *Comp. Phys. Comm.*, 151:60, 2003. <http://www.tddft.org/programs/octopus>.

- ¹⁹J. P. Perdew, K. Burke, and M. Ernzerhof. Generalized gradient approximation made simple. *Phys. Rev. Lett.*, 77:3865, 1996.
- ²⁰N. Troullier and J. L. Martins. Efficient pseudopotentials for plane-wave calculations. *Phys. Rev. B*, 43:1993, 1991.
- ²¹Ursula Rothlisberger and Wanda Andreoni. Structural and electronic properties of sodium microclusters ($n=2-20$) at low and high temperatures: New insights from ab initio molecular dynamics. *J. Chem. Phys.*, 94(12):8129, 1991.
- ²²M. E. Casida. *Recent Developments and Application of Modern Density Functional Theory*. Elsevier, Amsterdam, 1996.
- ²³J. P. Perdew and A. Zunger. Self-interaction correction to density-functional approximations for many-electron systems. *Phys. Rev. B*, 23:5048, 1981.
- ²⁴G. Huber, K.P.; Herzberg. *Molecular spectra and molecular structure. IV. constants of diatomic molecules*, 1979.
- ²⁵W. C. Martin and R. Zalubas. Energy levels of sodium, Na I through Na XI. *J. Phys. Chem.*, 10:153, 1981.
- ²⁶This is the minimum volume which we reproduces the free cluster results.
- ²⁷Balasaheb J. Nagare, Dilip G. Kanhere, and Sajeev Chacko. Structural and electronic properties of sodium clusters under confinement. *Phys. Rev. B*, 91:054112, 2015.
- ²⁸W. A. de Heer. The physics of simple metal clusters: experimental aspects and simple models. *Rev. Mod. Phys.*, 65:611, 1993.
- ²⁹H. Akeby, I. Panas, L. G. M. Pettersson, P. Siegbahn, and U. Wahlgren. Electronic and geometric structure of the Cu_n cluster anions ($n \leq 10$). *J. Phys. Chem.*, 94:5471, 1990.
- ³⁰Ilia A Solov'yov, Andrey V Solov'yov, and W. Greiner. Optical response of small magnesium clusters. *J. Phys. B: At. Mol. Opt. Phys.*, 37:L137, 2004.
- ³¹S. Pollack, C. R. C. Wang, and M. M. Kappes. On the optical response of Na_{20} and its relation to computational prediction. *J. Chem. Phys.*, 94:2496, 1991.
- ³²C. R. C. Wang, S. Pollack, T. A. Dahlseid, G. M. Koretsky, , and M. M. Kappes. Photodepletion probes of Na_5 , Na_6 , and Na_7 molecular dimensionality transition (2d-3d)? *J. Chem. Phys.*, 96:7931, 1992.
- ³³M. A. L. Marques, A. Castro, and A. Rubio. Assessment of exchange-correlation functionals for the calculation of dynamical properties of small clusters in time-dependent density functional theory. *J.*

- Chem. Phys.*, 115:3006, 2001.
- ³⁴I. Vasiliev, I. S. Ogut, and J. R. Chelikowsky. First-principles density-functional calculations for optical spectra of clusters and nanocrystals. *Phys. Rev. B*, 65:115416, 2002.
- ³⁵Juan C. Idrobo, Weronika Walkosz, Shing Fan Yip, Serdar Ogut, Jinlan Wang, and Julius Jellinek. Static polarizabilities and optical absorption spectra of gold clusters (Au_n , $n=2-14$ and 20) from first principles. *Phys. Rev. B*, 76:205422, 2007.
- ³⁶Satyender Goel, Kirill A. Velizhanin, Andrei Piryatinski, Sergei A. Ivanov, and Sergei Tretiak. Ligand effects on optical properties of small Gold clusters: A TDDFT study. *J. Phys. Chem. C*, 116:3242, 2012.
- ³⁷W. Rechberger, A. Hohenau, A. Leitner, J.R. Krenn, B. Lamprecht, and F.R. Ausseneg. Optical properties of two interacting gold nanoparticles. *Optics Communications*, 220:137, 2003.
- ³⁸L. J. Sham and M. Schluter. Density-functional theory of the energy gap. *Phys. Rev. Lett.*, 51:1888, 1983.
- ³⁹A. J. Cohen, P. Mori-Sanchez, and W. Yang. Fractional charge perspective on the band gap in density-functional theory. *Phys. Rev. B*, 77:115123, 2008.
- ⁴⁰W. R. Fredrickson and W. W. Watson. The sodium and potassium absorption bands. *Phys. Rev. B*, 30:429, 1927.
- ⁴¹Blanc, J and Bonačić-Koutecký, V and Broyer, M and Chevaleyre, J and Dugourd, Ph and Koutecký, J and Scheuch, C and Wolf, JP and Wöste, L. Evolution of the electronic structure of lithium clusters between four and eight atoms. *J. Chem. Phys.*, 96(3):1793, 1992.
- ⁴²V. Beutel, H.G. Kramer, G. L. Bhale, M. Kuhn, K. Weyers, and W. Demtroder. High-resolution isotope selective laser spectroscopy of Ag_2 molecules. *J. Chem. Phys.*, 98(4):2699, 1993.
- ⁴³Juzar Thingna, R. Prasad, and S. Auluck. Photo-absorption spectra of small hydrogenated silicon clusters using the time-dependent density functional theory.
- ⁴⁴W. D. A. M de Boer, D. Timmerman, K Dohnalova, I. N. Yassievich, H. Zhang, W. J. Buma, and T. Gregorkiewicz. Red spectral shift and enhanced quantum efficiency in photon-free photoluminescence from silicon nanocrystals. *Nat. Nanotech.*, 5:878, 2010.

TABLE I: Some of the features of dipole allowed excitation spectrum of sodium clusters in free space (V_0). Ionization Potential (I.P.), Excitation, Excitation Energy (E_{exc}), Energy of the most significant peak (E_m), HOMO-LUMO gap (E_g), Strength function [S_ω , (1/eV)], Optical gap (E_{gopt}) and excited state compositions. Only a selection of the most intense and representative transitions are considered.

Clusters	I.P.	Excitation	E_{exc}	E_m	S_ω	E_g	E_{gopt}	Excited state composition
Na ₂	5.57	1, 2	1.01, 2.12	1.86, 2.57	8.12, 12.57	1.01	1.83	i. 96.04% 3s→3p _x , 3.57% 3s→3d _{x²-y²} ii. 89.11% 3s→3p _z , 8.06% 3s→4p _y
Na ₃	4.22	6, 13, 19	1.48, 1.76, 2.39	1.85, 2.58, 3.00	6.28, 9.77, 9.29	0.50	0.70	i. 16.6% 3s→3p _x , 23.5% 3p _x →3d _{x²-y²} ii. 39.6% 3s→3p _x , 56.2% 3p _x →3d _{x²-y²} iii. 3.6% 3s→3p _x , 33.5% 3s→4s, 9.7% 3p _x →3d _{x²-y²}
Na ₄	4.57	4, 9, 15	i.1.90, 1.24, 2.18 ii.1.90, 1.84 iii. 2.44, 2.24, 3.55	1.91, 2.83, 3.13	10.63, 10.02, 10.11	0.71	1.82	i. 5.4% 3s→3p _y , 70% 3p _x →3p _z 11% 3p _x →3d _{xz} ii. 46% 3s→3p _y , 27% 3p _x →3d _{xy} iii. 56% 3s→4s, 11% 3p _x →3d _{x²-y²} , 26% 3p _y →5p _y
Na ₅	4.18	15, 24, 45	i.1.37, 2.07 ii. 1.51, 1.63, 2.07 iii. 2.63, 3.23	2.03,2.50, 3.23	10.54, 10.92, 10.05	0.86	1.05	i. 52% 3p _x →3p _z , 64% 3p _x →3d _{xz} ii. 40% 3s→3p _y , 26% 3p _x →3d _{xy} iii. 48% 3s→4s, 42% 3p _y →4f _{xyz}
Na ₆	4.73	24	1.37, 1.61	2.34	50.11	1.12	1.26	15.80%, 3p _y →4s, 14.90% 3p _y →3d _{xz}
Na ₇	3.16	34, 38, 64	i. 1.54, 2.26 ii. 1.54, 1.44 iii. 3.29, 3.30	2.42, 2.63, 3.21	9.94, 24.43, 11.93	0.95	0.91	i. 4.50% 3p _y →4s, 81.90% 3p _y →3d _{z²} ii. 9.5% 3p _x →4s, 12.4% 3p _z →3d _{yz} iii. 71.23% 3p _z →4f _{xyz} , 21.90% 3p _z →4f _{x(z²-y²)}
Na ₈	4.69	53	2.97, 2.96	2.82	36.89	1.30	1.50	45.02% 3p _y → 4d _{xz} and 50.06% 3p _z → 4d _{yz}
Na ₉	3.60	63, 88	i. 1.60, 2.72, 2.96 ii. 1.81, 3.01, 3.02	2.68, 2.96	30.68, 19.98	0.31	0.18	i. 9.15% 3p _x →3d _{xy} , 19.2% 4s→4f _{y(z²-x²)} , 10.8% 4s→4f _{x³} ii. 3.3% 3p _y →3d _{yz} , 13.52% 3p _z →4d _{z³} , 52.18% 4s→4f _{z³}
Na ₁₀	4.15	70, 107	i. 1.32, 1.29, 2.14 ii. 1.80, 1.62, 3.43	2.49, 3.05	21.56, 55.76	0.57	1.48	i. 16.90% 3p _y →3d _{xy} , 22.00% 4s→4p _x , 25.92% 4s→4d _{xy} ii. 6.47% 3p _x →3d _{xy} , 10.03% 3p _z →3d _{yz} , 15.80% 4s→5d _{xz}
Na ₁₁	3.54	83, 122	i. 1.26, 2.66, 2.71 ii. 2.95, 2.89, 2.96	2.55, 2.91	6.99, 7.20	0.49	1.31	i. 4.59% 4s→5p _x , 11.80% 3p _y →4p _z , 13.06% 3p _z →4p _z ii. 15.34% 3s→3d _{xz} , 20.73% 3p _z →4d _{xz} , 18.97% 3p _z →4d _{x²-y²}
Na ₁₂	4.23	84, 118	i. 2.21, 1.31, 2.31 ii. 1.49, 2.58, 1.51	2.36, 2.78	7.58, 8.19	0.76	0.70	i.3.32% 3p _x →3d _{yz} , 6.84% 3p _z →3d _{x²-y²} , 38.01% 3p _z →4d _{yz} ii. 8.02% 3p _y →3d _{xy} , 13.83% 3p _x →4p _x , 8.73% 3d _{xy} →4p _x
Na ₁₃	3.83	102, 136	i. 1.13, 1.29, 2.52 ii. 1.39, 2.76, 2.78	2.40, 2.71	16.17, 10.27	0.40	0.65	i. 5.64% 3p _z →3d _{yz} , 16.35% 4s→4p _x , 20.22% 4s→5p _y ii. 2.10% 3d _{xy} →4p _y , 13.93% 3p _z →5p _y , 67.74% 3d _{xz} →4f _{x³}
Na ₁₄	4.04	117, 147, 208	i. 2.38, 1.18, 2.52 ii. 2.47, 2.59, 2.55	2.40, 2.64	17.77, 12.44	0.82	1.12	i. 4.9% 3p _x →3d _{z²} , 7.2% 3d _{xy} →3d _{z²} , 20.2% 3d _{xz} →4f _{xyz} ii. 3.2% 3p _y →4p _y , 22.8% 3d _{xz} →4p _y , 22.4% 3d _{xz} →4f _{x(z²-y²)}
Na ₁₅	3.81	144, 161	i. 2.48, 2.53, 2.51 ii. 2.63, 2.74, 2.65	2.49, 2.65	12.67, 13.68	0.51	0.4	i. 9.5% 3p _x →3d _{z²} , 17.28% 3p _z →4d _{x²-y²} , 63.84% 3d _{xy} →4f _{xyz} ii. 8.0% 3p _x →4p _y , 20.15% 3p _x →5s, 10.58% 3p _z →4d _{z²}
Na ₁₆	3.99	195	2.56, 2.70, 2.75, 2.68	2.74	12.87	0.59	1.32	3.48% 3p _x →4p _y , 17.45% 3p _z →4d _{z²} , 55.54% 4s→4f _{z(x²-y²)} , 5.05% 3d _{xz} →4f _{x³}
Na ₁₇	4.11	225, 264	i. 2.80, 2.83, 2.84 ii. 1.74, 1.52, 1.59	2.82, 3.07	67.92, 39.47	0.46	0.92	i. 25.2% 3p _y →4d _{yz} , 21.7% 4s→4f _{z(x²-y²)} , 45.9% 3d _{xy} →4f _{x³} ii. 12.1% 3p _z →3d _{z²} , 6.4% 3d _{xy} →4d _{xy} , 8.02% 3d _{yz} →4d _{x²-y²} 4p _z
Na ₁₈	4.18	229	2.70, 2.77, 2.80	2.77	19.45	0.54	1.12	10.76% 3d _{yz} →4d _{x²-y²} , 10.12% 3d _{xz} →4f _{z³} , 32.64% 3d _{yz} →5d _{xz}
Na ₁₉	3.69	256, 289	i. 2.76, 2.72, 2.78 ii. 2.66, 2.70, 2.96	2.76, 2.89	32.08, 43.45	0.58	0.65	i. 7.32% 3p _x →4d _{xy} , 13.20% 3p _y →4d _{x²-y²} , 36.63% 3d _{xz} →5d _{xy} ii. 3.38% 3p _x →4p _y , 6.26% 3p _y →4f _{z(x²-y²)} , 9.15% 3d _{xy} →5d _{xz}
Na ₂₀	4.08	135, 158	i. 2.56, 2.63, 2.75 ii. 2.56, 2.78, 2.75	2.70, 2.88	44.09, 25.04	0.78	0.93	i. 16.82% 3p _x →5s, 5.05% 3p _x →4d _{xz} , 19.84% 4s→4f _{z³} ii. 4.56% 3p _x →5s, 19.34% 3p _y →5s, 11.71% 4s→4f _{z³}

TABLE II: Some of the features of dipole allowed excitation spectrum of sodium clusters under confined geometries (V_h). Ionization Potential (I.P.), Excitation, Excitation Energy (E_{exc}), Energy of the most significant peak (E_m), HOMO-LUMO gap (E_g), Strength function [S_ω , (1/eV)], Optical gap (E_{gopt}) and excited state compositions. Only a selection of the most intense and representative transitions are considered.

Clusters	I.P.	Excitation	E_{exc}	E_m	S_ω	g	E_{gopt}	Excited state composition
Na ₂	4.33	1, 2	1.61, 2.43	2.57, 3.19	7.50, 16.25	1.59	2.53	i. 99.40% 3s→3p _x ii. 75.69% 3s→3p _y 23.37% 3s→3p _z
Na ₃	3.16	8, 10, 12	2.50, 2.79, 2.70	2.51, 3.32, 3.76	1.98, 20.17, 14.39	0.27	1.58	i. 54.7% 3p _x →3d _{xy} , 41.9% 3p _x →3d _{x²-y²} ii. 20.79% 3p _x →3d _{xy} , 42.2% 3p _x →3d _{yz} iii. 40.7% 3s→3p _z , 16.8% 3p _x →3d _{xz}
Na ₄	3.47	7, 10	i. 2.19, 1.97 ii. 2.68, 2.65	3.73, 4.10	21.61, 24.43	0.52	1.90	i. 55% 3s→3p _y , 41% 3p _x →4s ii. 57% 3s→3p _z , 40% 3p _x →3d _{xy}
Na ₅	2.90	22, 31	i. 1.99, 2.32 ii. 2.72, 2.65	3.62, 4.27	17.92, 24.99	0.96	1.84	32% 3p _x →4s 60% 3p _y →3d _{xy} ii. 46% 3s→3p _z , 32% 3p _x →3d _{xz}
Na ₆	3.88	33	2.90, 2.91	2.62	50.56	1.18	1.32	26.06%, 3p _y →3d _{z²} , 9.68%, 3p _y →4p _x
Na ₇	3.44	31, 41, 61	i. 1.66, 3.05 ii. 3.05, 3.06 iii. 2.12, 1.80	2.58, 2.92, 3.41	5.71, 37.85, 23.42	1.34	1.05	i. 12.6% 3p _x →3d _{z²} , 16.8% 3p _y →3d _{z²} ii. 10.24% 3p _x →3d _{xy} , 16.8% 3p _y →4p _y iii. 43.80% 3s→3p _z , 23.78% 3p _z →3d _{z²}
Na ₈	4.15	60	1.78, 2.07, 3.28	3.54	89.92	1.80	1.62	15.3% 3p _x →3d _{yz} , 21.9% 3p _y →4p _x , 16.7% 3p _z →3d _{xy}
Na ₉	2.89	63, 72	i. 1.48, 3.54, 3.55 ii. 1.88, 4.01, 3.71	3.58, 3.72	36.50, 30.06	0.25	0.21	i. 5.18% 3p _z →3d _{xy} , 5.52% 3p _x →4p _y , 13.5% 3p _z →5s ii. 4.86% 3p _x →3d _{xy} , 11.52% 3p _y →4d _{xy} , 8% 3p _z →4d _{yz}
Na ₁₀	2.54	101, 109	i. 2.05, 0.90, 4.06 ii. 1.39, 3.45, 3.50	3.94, 4.22	72.43, 31.62	0.17	2.23	i. 5.64% 3p _x →3d _{xz} , 6.48% 4s→3d _{z²} , 40.70% 3p _x →5s ii. 6.26% 3p _y →3d _{xy} , 27.23% 4s→4d _{z²} , 41.40% 4s→5p _x
Na ₁₁	2.42	101, 124	i. 4.59, 4.75, 4.73 ii. 4.59, 5.09, 4.90	4.64, 5.12	9.18, 5.73	0.16	2.01	i. 6.55% 3s→3d _{x²-y²} , 21.38% 3p _x →5s, 18.60% 3p _y →4d _{xz} ii. 3.97% 3s→3d _{x²-y²} , 3.43% 3p _y →4d _{yz} , 27.38% 3d _{xy} →4f _{xyz}
Na ₁₂	2.08	120	5.12, 4.96, 4.89	4.94	14.75	0.44	1.26	2.46% 3s→4p _x , 22.84% 3p _x →5s, 14.47% 3p _z →4d _{yz}
Na ₁₃	2.10	143, 155	i. 3.90, 3.92, 3.98 ii. 1.94, 2.04, 4.13	3.90, 4.03	19.45, 24.75	0.18	1.08	i. 8.9% 3s→3d _{x²-y²} , 12.2% 3s→3d _{z²} , 20.7% 3p _y →4d _{yz} ii. 8% 3p _y →3d _{yz} , 13.5% 3p _z →3d _{z²} , 23.6% 3d _{xz} →4f _{z(x²-y²)}
Na ₁₄	2.54	148, 166, 177	i. 3.64, 3.95 ii. 2.08, 4.17 iii. 2.08	3.86, 4.13, 4.31	8.38, 22.87, 20.46	0.35	1.27	i. 2.1% 3p _x →4d _{yz} , 80.3% 3p _z →4d _{z²} ii. 2.8% 3p _z →3d _{yz} , 18.9% 3p _x →4d _{yz} iii. 5.51%, 3p _z →3d _{z²}
Na ₁₅	2.31	167, 190	i. 3.96, 3.84 ii. 2.05, 4.20	3.91, 4.22	11.82, 34.63	0.23	1.04	i. 4.08% 3p _x →4d _{xz} , 11.8% 3p _z →4d _{x²-y²} , 17.6% 3d _{yz} →4f _{z(x²-y²)} ii. 13.7% 3d _{xz} →4f _{x³} , 23.1% 3d _{yz} →4f _{x(z²-y²)}
Na ₁₆	2.14	202	4.24, 4.13, 4.22, 4.14	4.16	31.85	0.28	1.51	3.86% 3p _y →4d _{x²-y²} , 7.68% 3p _z →4d _{x²-y²} , 13.10% 3d _{xz} →4f _{z(x²-y²)} , 6.84% 3d _{xz} 4f _{x³}
Na ₁₇	1.56	236, 248	i. 2.27, 1.91, 4.27 ii. 2.45, 1.86, 4.01	4.21, 4.29	81.91, 57.72	0.27	1.17	i. 8.04% 3p _z →3d _{z²} , 11.8% 3d _{xy} →4d _{xz} , 11.9% 3p _x →4d _{z²} ii. 2.04% 3p _x →3d _{z²} , 7.9% 4s→4p _z , 15.2% 3d _{xy} →4f _{z(x²-y²)}
Na ₁₈	2.07	260	4.24, 4.35, 4.37	4.35	33.20	0.38	1.55	4.80% 3s→4p _x , 14.25% 3d _{xy} →4f _{x³} , 12.20% 3d _{x²-y²} →5d _{yz}
Na ₁₉	1.71	277	4.41, 4.22, 4.25, 4.42	4.33	64.89	0.60	0.82	5.57% 3s→4p _y , 11.71% 4s→4f _{z(x²-y²)} , 27.25% 3d _{xy} →4f _{x³} , 23.80% 3d _{xz} →5d _{xy}
Na ₂₀	1.25	140	1.89, 4.45, 1.91, 2.26	4.33	64.22	0.54	1.02	6.48% 4s→4p _y , 4.62% 3s→4p _z , 8.42% 3d _{xz} →5s, 12.80% 3d _{x²-y²} →5p _x



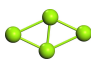
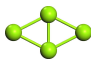
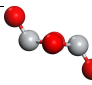
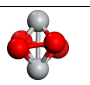
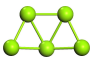
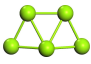
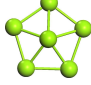
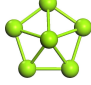



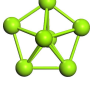
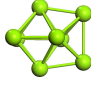
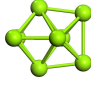



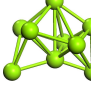
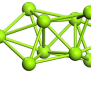
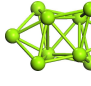
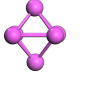
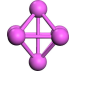
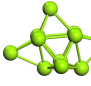
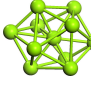
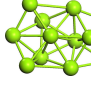
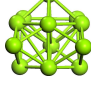
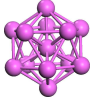
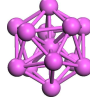
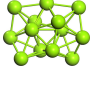
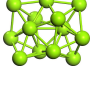
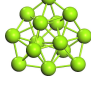
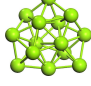


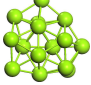
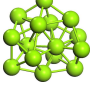
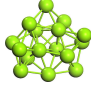
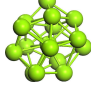

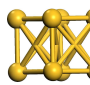
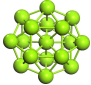
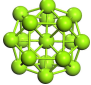
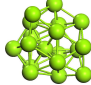
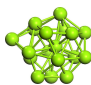
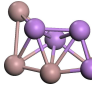
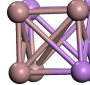
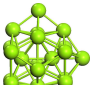
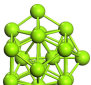
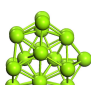

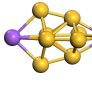
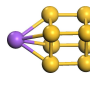
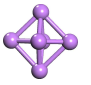
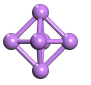
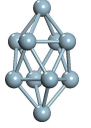
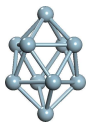
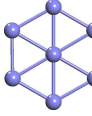
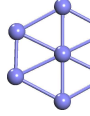
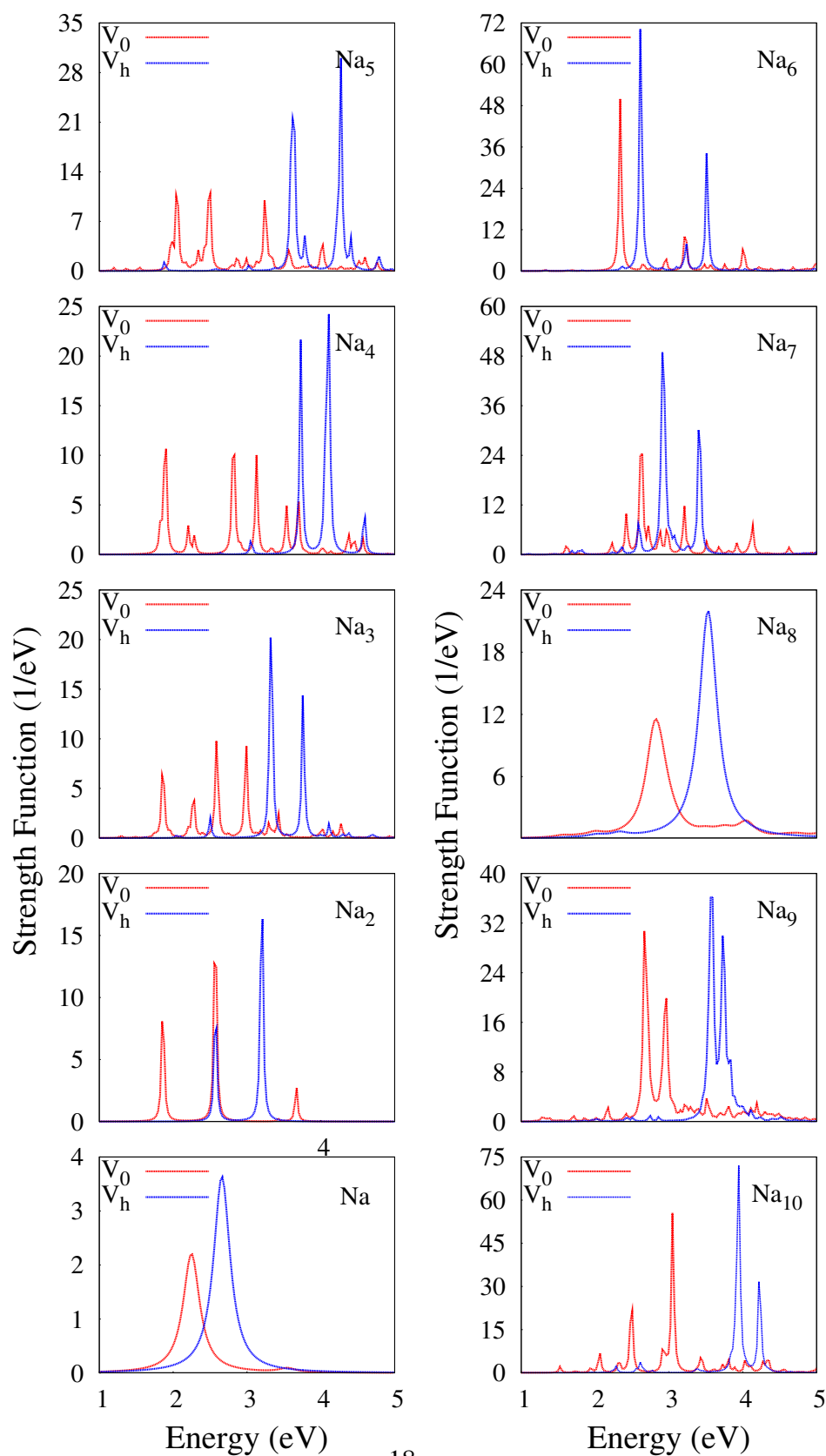
Lowest Equilibrium Structures									
Clusters	V_0	V_h	Clusters	V_0	V_h	Clusters	V_0	V_h	
Na_3	 -17.069	 -16.134	Na_4	 -23.449	 -21.436	Ti_2O_4	 -1941.696	 -1896.064	
Na_5	 -29.417	 -26.166	Na_6	 -35.961	 -32.174	Ag_2	 -19.098	 -15.161	
Na_7	 -42.254	 -38.920	Na_8	 -48.663	 -43.287	Ag_3	 -29.441	 -19.945	
Na_9	 -54.539	 -48.364	Na_{10}	 -61.008	 -57.927	Al_6	 -333.025	 -317.996	
Na_{11}	 -66.795	 -57.445	Na_{12}	 -73.215	 -69.097	Al_{13}	 -729.524	 -654.143	
Na_{13}	 -79.779	 -76.697	Na_{14}	 -86.340	 -84.829	Si_4	 -424.682	 -417.309	
Na_{15}	 -92.430	 -90.832	Na_{16}	 -98.838	 -92.787	Si_8	 -853.018	 -850.110	
Na_{17}	 -105.125	 -99.479	Na_{18}	 -111.716	 -103.133	Ga_4As_4	 -934.927	 -905.796	
Na_{19}	 -118.214	 -108.851	Na_{20}	 -124.762	 -122.854	Si_6Na_2	 -868.978	 -825.006	
Li_6	 -37.806	 -35.825	K_{10}	 -104.997	 -102.318	Cs_7	 -599.223	 -593.036	

FIG. 1: The geometries of the lowest equilibrium structures of various metallic and semiconductor nanoclusters along with their total energies in eV. In each of cases, the second and fifth row represent free clusters, whereas third and sixth row present confined geometries. The V_0 and V_h denote the free and highest compressed state.



18

FIG. 2: Photoabsorption spectra of lowest equilibrium structures of Na_n clusters with $n=2-10$ in confined geometries. Note the different scalings of the axes of ordinates. The symbols V_0 and V_h have same meaning as mentioned above.

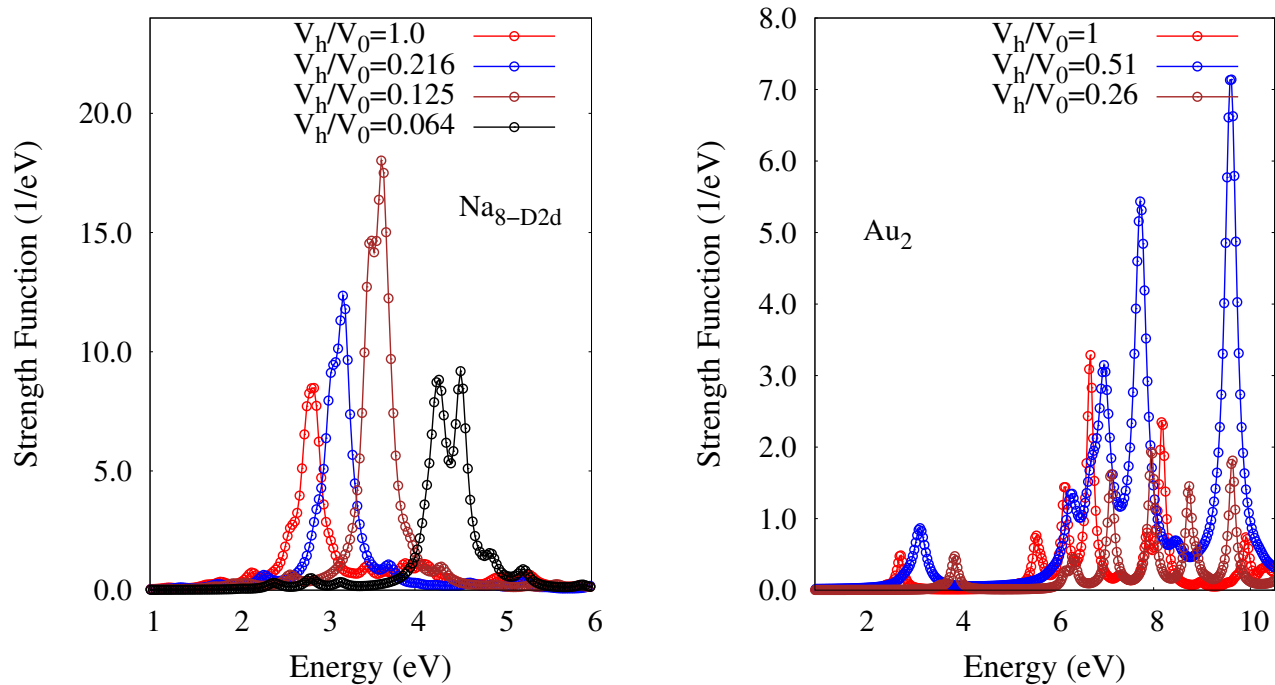


FIG. 3: Photoabsorption spectra of the lowest equilibrium structures of $\text{Na}_8\text{-D}_{2d}$ and Au_2 clusters at various compressions. Note the different scalings of the axes of ordinates.

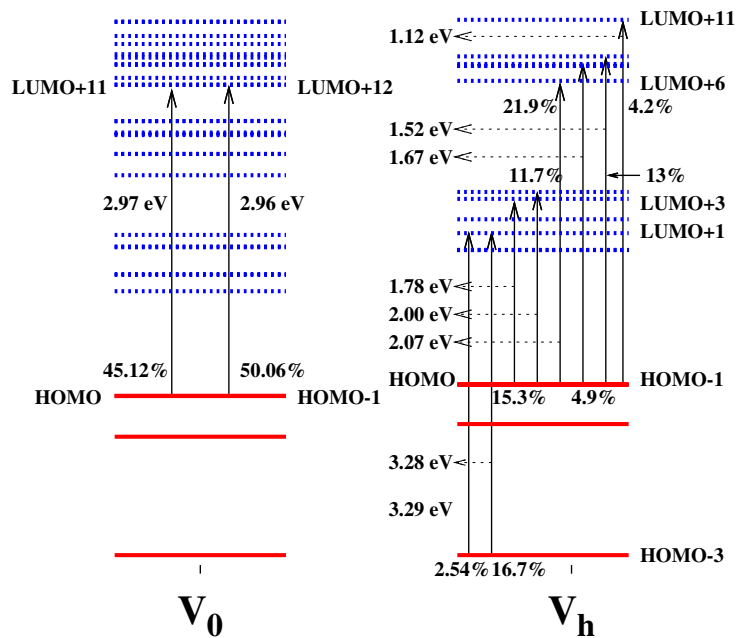


FIG. 5: Energy level diagram of the major energy excitation at energy $E=2.82$ and 3.54 eV in free and confined space respectively.

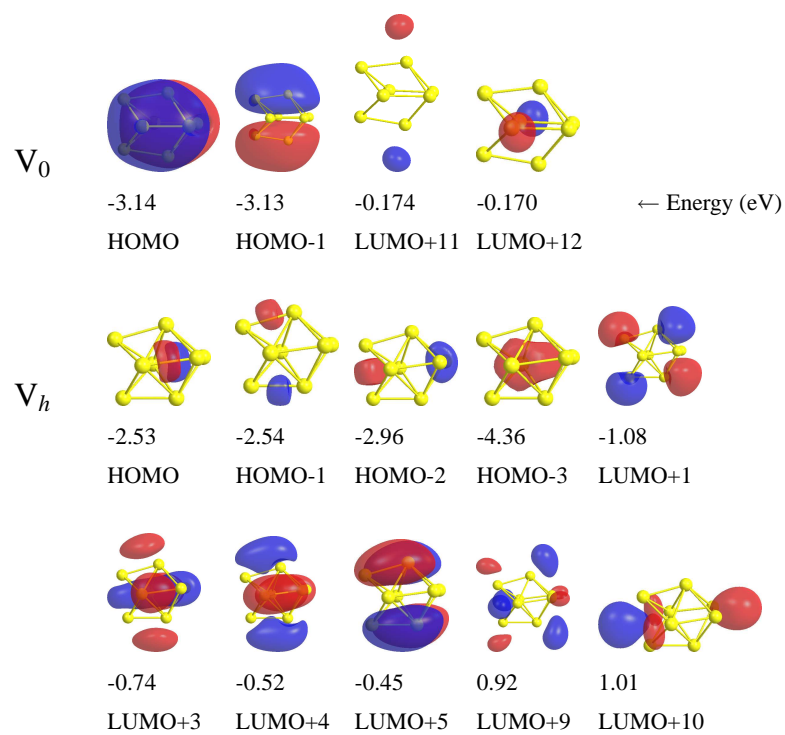
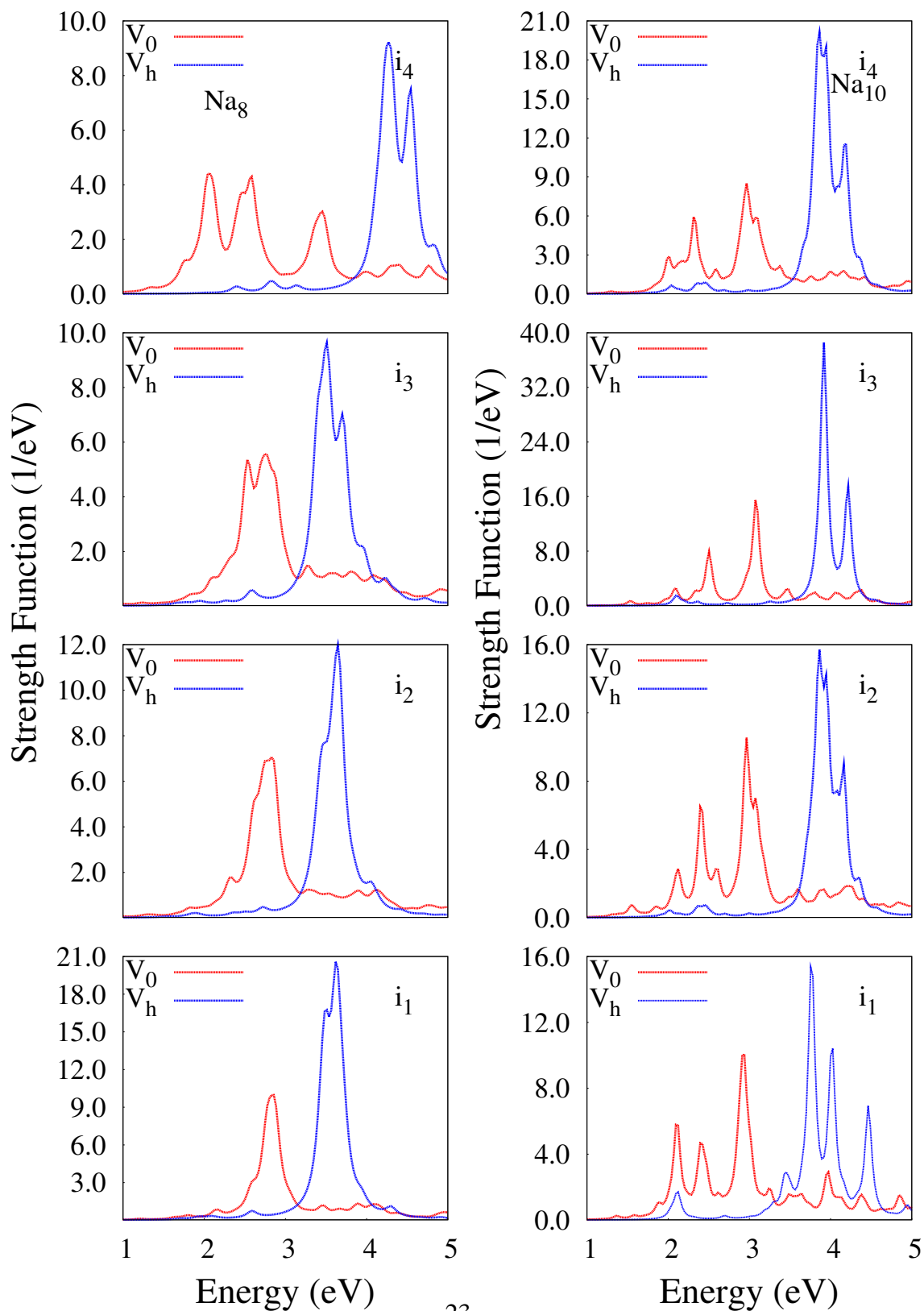


FIG. 6: Orbital illustrations of Na_8 clusters. Dark blue represents positive and red negative parts of the wavefunctions. All isovalues are plotted at $1/3^{\text{rd}}$ of total isovalue.



23

FIG. 7: Photoabsorption spectra of low lying isomers of Na_8 and Na_{10} clusters at V_0 and V_h . Note the different scalings of the axes of ordinates.

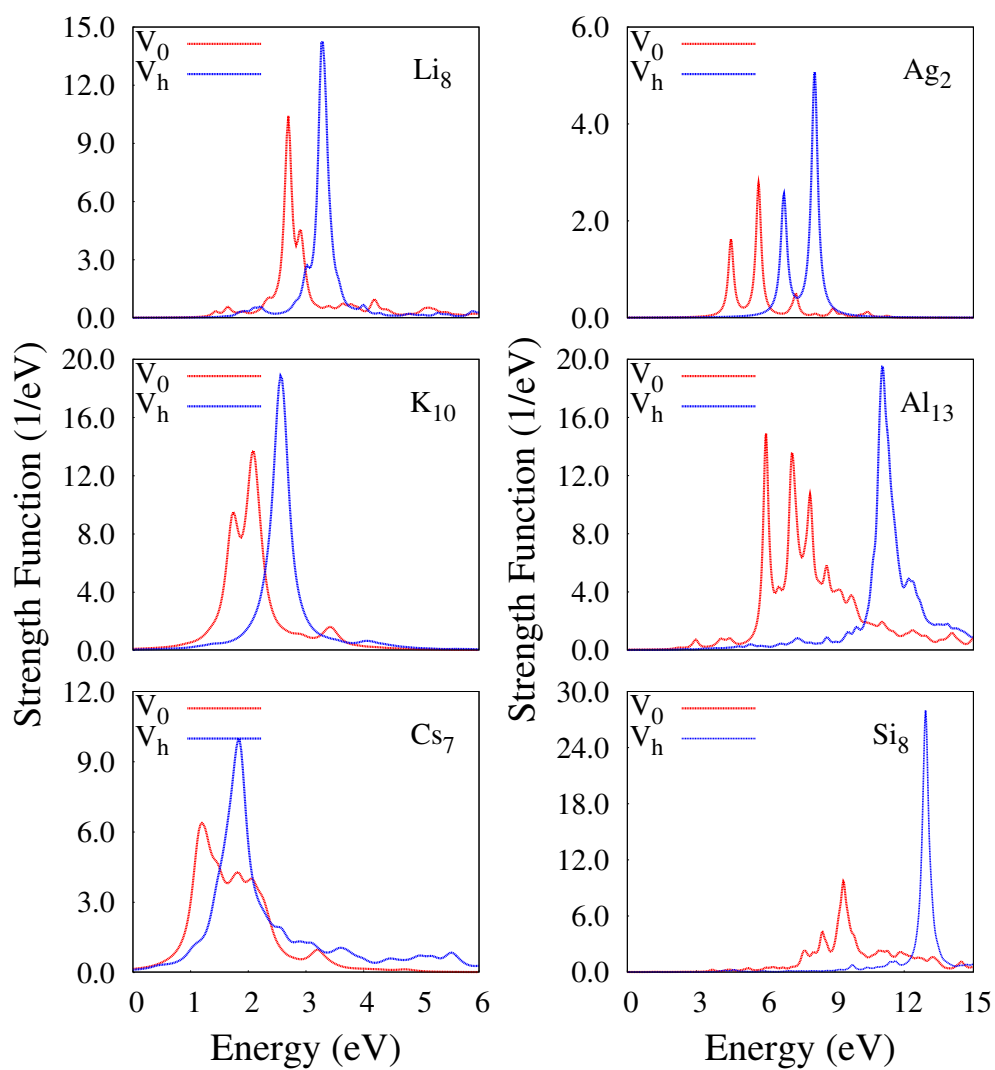


FIG. 8: Photoabsorption spectra of lowest equilibrium structures of some of the nanoclusters at V_0 and V_h . Note the different scalings of the axes of ordinates.